

Theory and experiments on multiwave-mixing-mediated probe-beam amplification

I. C. Khoo and T. H. Liu*

Department of Electrical Engineering, The Pennsylvania State University, University Park, Pennsylvania 16802

(Received 1 July 1988; revised manuscript received 3 November 1988)

In a highly nonlinear thin film, the presence of the diffracted beams from the pump-probe-beam-induced refractive-index grating modifies considerably the energy coupling between the pump and the probe beams. Using coupled amplitude and phase equations, the roles of various factors such as phases and phase shifts, phase modulations, pump-beam intensity, intensity ratio, interaction length, and losses in the medium in the multiwave-mixing processes are clearly identified. We also present experimental results on the dependence of the probe gain on the pump-probe-beam ratio, the pump intensity, and on the interaction length, using a nematic liquid-crystal film as the nonlinear medium.

INTRODUCTION

Recently, with the emergence of several highly nonlinear materials, the theory and practice of nonlinear optical processes have assumed several new, interesting and potentially useful forms. The successes by several research groups in fabricating thin film bistable optical elements,¹ electro-optical devices,² and observing new wave-mixing effects³ are but a few examples. In particular, theories and experiments on degenerate optical wave mixings in highly nonlinear media such as liquid crystals⁴ and semiconductors⁵ have demonstrated the profound effect that the often neglected diffracted beam will have on the usual pump-probe wave-mixing processes.

Referring to Fig. 1, which depicts schematically the interaction of two coherent cw laser beams in a nonlinear medium, the diffracted beams (E_3 and E_4) are generated by the refractive-index grating induced by the intensity interference grating formed by the two incident lasers. In general, the probe beam E_2 is very weak compared to the pump beam E_1 , giving rise to very small intensity (and therefore index) modulation; this gives rise to a very weak diffracted beam E_3 and an even weaker beam E_4 . In many studies except a few,⁶⁻¹¹ these diffracted beams are usually neglected and one is concerned with only the interaction between beam 1 and beam 2. In the context of the amplification of the weak probe beam E_2 by the strong pump beam E_1 , studies have shown that the probe beam E_2 will experience gain provided that (i) it is Stokes shifted in frequency with respect to the pump beams, i.e., Ω is negative (in general, Ω should be on the order of the inverse of the relaxation time of the nonlinear medium response), or (ii) if $\Omega=0$, the medium possesses a nonlocal response, where the refractive index grating is phase shifted relative to the intensity grating. These processes are usually referred to as two-wave-mixing processes, and have generally been observed in photorefractive crystals.

When $\Omega=0$, i.e., the strictly degenerate case, amplification of the probe beam can occur via multiwave mixing involving the diffracted beam. As schematically

depicted in Fig. 1(b), the pump beam 1 can interfere with the diffracted beam 3, which then scatters the beam 1 into the probe beam 2 direction. This provides therefore a gain mechanism to the probe. On the other hand, there is a counterpart process in which beam 2 and beam 4 interfere with one another and scatter light into the beam 1 direction. Thus amplification of the probe beam 2 will occur if it is weaker than beam 1. Amplification of a weak probe beam by a strong pump beam has been studied in various contexts. However, these theories and experiments have been concentrated mainly on problems where only the diffracted beam 3 is taken into account.^{5(a),12,13} This corresponds to the case of very large pump-to-probe beam ratio. If beam 2 substantially amplified, for example, by a factor of 10 or so, this assumption of a very large pump-to-probe beam ratio may no longer hold (an experimentally proven fact), and the role of beam 4 becomes very important.

In this paper the multiwave-mixing effects (e.g., probe-beam gain) reported in Ref. 4 are quantitatively described by a coupled-phase-and-amplitude-equations approach that accounts for all relevant interacting laser beams. This new theoretical framework provides new valuable insights. We will also present some new experimental results. Specifically, we will show how the complex coupled equations may be reduced to a simple set of input variables, and the amplification or depletion of beams are governed by the pump intensity, the strong intensity-dependent phases and phase shifts, and the role of all the diffracted beams as well as medium losses. Experiments with the giant orientational nonlinearity of nematic liquid crystal films will illustrate some of the general points, and also specific experimental details for achieving high gain and eliminating unwanted effects.

THEORY

Consider again the interaction geometry as depicted in Fig. 1. The Maxwell equation governing the propagation of the electromagnetic wave in the nonlinear medium is given by⁶

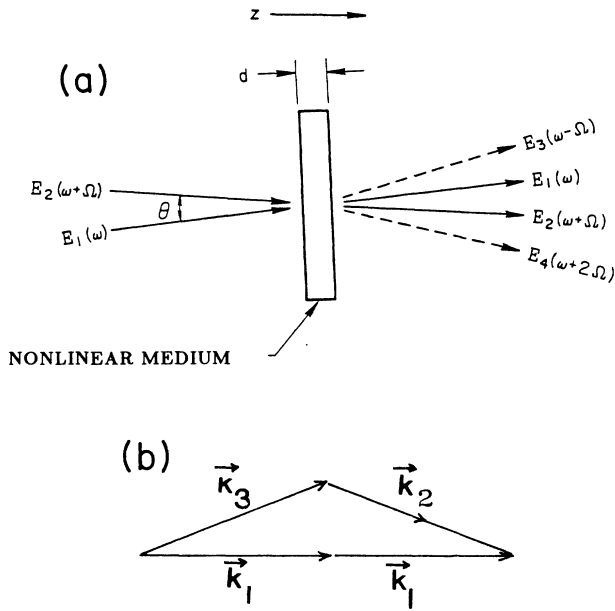


FIG. 1. (a) Schematic diagram of the mixing of a pump (1) and a probe (2) beam in a nonlinear medium. Beams 3 and 4 are diffractions of the pump and the probe beam from the index grating created by the pump-probe interference. (b) Schematic of the mixing of beams 1 and 3 to provide gain in the beam-2 direction.

$$\nabla^2 E - \mu_0 \epsilon \frac{\partial^2 E}{\partial t^2} = \mu_0 \frac{\partial^2 P_{NL}}{\partial t^2}, \quad (1)$$

where the nonlinear polarization P_{NL} , assumed of the third-order form, is given by

$$P_{NL}^i = 4\chi_{ijkl} E^j E^k E^l, \quad (2)$$

where χ_{ijkl} is the third-order nonlinear susceptibility and the subscripts and superscripts represent the Cartesian coordinates. For degenerate optical wave mixing (i.e., all frequencies are the same) and assuming for simplicity that all fields are polarized in the same direction, we may write χ_{ijkl} as $\chi^{(3)}$, which is related to the Kerr coefficient n_2 by

$$\chi^{(3)} = \frac{1}{3} \epsilon_0 n_0 n_2 \quad (3)$$

and the Kerr coefficient is defined by the effective refractive index of the nonlinear medium n by

$$\begin{aligned} n &= n_0 + n_2 \langle E^2 \rangle \\ &= n_0 + n_2 I, \end{aligned} \quad (4)$$

where n_0 is the linear (under zero optical field) refractive index of the medium.

Using the plane-wave approximations for the optical electric field and the polarization, respectively,

$$\mathbf{E}_j = \frac{1}{2} \hat{\mathbf{x}} [E_j \exp(i(\omega t - k_{zj}z) + \text{c.c.})], \quad (5)$$

$$\mathbf{P}_j = \frac{1}{2} \hat{\mathbf{x}} [P_j \exp(i(\omega t - k_{zj}z) + \text{c.c.})], \quad j = 1, 2, 3, 4 \quad (6)$$

and the slowly varying envelope approximation

$$|k^2 E| \gg \left| k \frac{\partial E}{\partial Z} \right| \gg \left| \frac{\partial^2 E}{\partial Z^2} \right|, \quad (7)$$

one can combine Eqs. (1) and (2) to give the following equations:

$$\begin{aligned} \frac{dE_1}{dz} &= -ig(|E_1|^2 + 2|E_2|^2 + 2|E_4|^2)E_1 \\ &\quad -ig\{E_2^2 E_4^* \exp[i(-3\phi - \Delta k_3 z)] \\ &\quad + E_2^* E_3 E_4 \exp[2i\Delta k_3 z] \\ &\quad + E_1^* E_2 E_3 \exp[i\Delta k_3 z]\} - \frac{1}{2}\alpha E_1, \end{aligned} \quad (8)$$

$$\begin{aligned} \frac{dE_2}{dz} &= -ig(|E_2|^2 + 2|E_1|^2 + 2|E_3|^2 + 2|E_4|^2)E_2 \\ &\quad -ig[E_1^2 E_3^* \exp(-i\Delta k_3 z) + E_1 E_4 E_2^* \exp(i\Delta k_3 z) \\ &\quad + E_3 E_4 E_1^* \exp(2\Delta k_3 z)] - \frac{1}{2}\alpha E_2, \end{aligned} \quad (9)$$

$$\begin{aligned} \frac{dE_3}{dz} &= -ig(|E_3|^2 + 2|E_1|^2 + 2|E_2|^2 + 2|E_4|^2)E_3 \\ &\quad -ig\{E_1^2 E_2^* \exp[-i(\phi + \Delta k_3 z)] \\ &\quad + E_1 E_2 E_4^* \exp[-2i\Delta k_3 z]\} - \frac{1}{2}\alpha E_3, \end{aligned} \quad (10)$$

$$\begin{aligned} \frac{dE_4}{dz} &= -ig(|E_4|^2 + 2|E_1|^2 + 2|E_2|^2 + 2|E_3|^2)E_4 \\ &\quad -ig\{E_2^2 E_1^* \exp[i(\phi - \Delta k_3 z)] \\ &\quad + E_1 E_2 E_3^* \exp[-2i\Delta k_3 z]\} - \frac{1}{2}\alpha E_4, \end{aligned} \quad (11)$$

where $\Delta k_3 = 2k_1 - k_2 - k_3$ and α is the intensity loss constant.

In Eqs. (1)–(4), E_j 's are the complex amplitude of the electric field \mathbf{E}_j

$$E_j = \frac{1}{2} [E_j \exp(i(\omega_j t - k_j z) + \text{c.c.})]. \quad (12)$$

The coupling constant g is defined by

$$g = \frac{\omega^2 n_0 n_2}{2kc^2}.$$

In order to study the roles played by the intensities and phases of the optical fields, we rewrite these complex electric field amplitude equations into *real amplitude* $\sqrt{I_j}$ and *phase* (ϕ_j) equations by redefining E_j as

$$E_j = (2\sqrt{\mu/\epsilon})^{1/2} \sqrt{I_j} \exp(i\phi_j), \quad j = 1, \dots, 4. \quad (13)$$

Using (13) in Eq. (8)–(11), and after some straightforward but cumbersome algebra, we obtain the following equations.

(i) *Amplitude equations.*

$$\begin{aligned} \frac{dI_1}{dz} = & 4g' \sin\phi(-I_1I_2 + I_1I_3 - I_1I_4) + 2gI_2\sqrt{I_1I_4} \sin(\phi_{24} + \phi_{21} - 3\phi - \Delta k_3 - \phi_{2z}) \\ & + 2g'I_1\sqrt{I_2I_3}[\sin(\phi_{21} + \phi_{31} - \phi) + \Delta k_3z + \sin(\phi_{21} + \phi_{31} + 3\phi + \Delta k_3z)] \\ & + 2g'\sqrt{I_1I_2I_3I_4}[\sin(\phi_{31} + \phi_{42} - 2\phi + 2\Delta k_3z) + \sin(\phi_{31} + \phi_{42} + \phi + 2\Delta k_3z)] - \alpha I_1, \end{aligned} \quad (14)$$

$$\begin{aligned} \frac{dI_2}{dz} = & 4g'I_2(I_1 \sin\phi + I_3 \sin 2\phi - I_4 \sin\phi) + 2gI_1\sqrt{I_2I_3} \sin(\phi_{12} + \phi_{13} - \Delta k_3 + \phi) \\ & + 2g'I_2\sqrt{I_1I_4}[\sin(\phi_{12} + \phi_{42} + \Delta k_3z + 3\phi) + \sin(\phi_{12} + \phi_{42} + \Delta k_3z - \phi)] \\ & + 2g'\sqrt{I_1I_2I_3I_4}[\sin(\phi_{31} + \phi_{42} + 2\Delta k_3z + 2\phi) + \sin(\phi_{31} + \phi_{42} + 2\Delta k_3z - \phi)] - \alpha I_2, \end{aligned} \quad (15)$$

$$\begin{aligned} \frac{dI_3}{dz} = & 4g'(-I_1I_3 \sin\phi - I_2I_3 \sin 2\phi - I_4I_3 \sin 3\phi) + 2gI_1\sqrt{I_2I_3}[\sin(\phi_{13} + \phi_{12} - \phi - \Delta k_3z)] \\ & + 2g'\sqrt{I_1I_2I_3I_4}[\sin(\phi_{13} + \phi_{24} - \phi - 2\Delta k_3z) + \sin(\phi_{13} + \phi_{24} - 2\phi - 2\Delta k_3z)] - \alpha I_3, \end{aligned} \quad (16)$$

and

$$\begin{aligned} \frac{dI_4}{dz} = & 4g'(I_4I_1 \sin 2\phi + I_4I_2 \sin\phi + I_3I_4 \sin 3\phi) + 2gI_2\sqrt{I_1I_4} \sin(\phi_{21} + \phi_{24} + \phi - \Delta k_3z) \\ & + 2g'\sqrt{I_1I_2I_3I_4}[\sin(\phi_{13} + \phi_{24} + \phi - 2\Delta k_3z) + \sin(\phi_{13} + \phi_{24} + 2\phi - 2\Delta k_3z)] - \alpha I_4, \end{aligned} \quad (17)$$

where α is the linear loss of the medium (due to, e.g., absorption, scattering, etc.).

(ii) *Phase equations.*

$$\begin{aligned} \frac{d\phi_1}{dz} = & -g'(I_1 + 2I_2 \cos\phi + 2I_3 \cos\phi + 2I_4 \cos 2\phi) - gI_2\sqrt{I_4/I_1}[\cos(\phi_{24} + \phi_{21} - 3\phi - \Delta k_3z)] \\ & - g'\sqrt{I_2I_3}[\cos(\phi_{21} + \phi_{31} - \phi + \Delta k_3z) + \cos(\phi_{21} + \phi_{31} + 3\phi + \Delta k_3z)] \\ & - g'\frac{\sqrt{I_2I_3I_4}}{I_1}[\cos(\phi_{31} + \phi_{42} - 2\phi + 2\Delta k_3z) + \cos(\phi_{31} + \phi_{42} + \phi + 2\Delta k_3z)], \end{aligned} \quad (18)$$

$$\begin{aligned} \frac{d\phi_2}{dz} = & -g'(I_2 + 2I_1 \cos\phi + 2I_3 \cos 2\phi + 2I_4 \cos\phi) - gI_1\frac{\sqrt{I_3}}{I_2} \cos(\phi_{12} + \phi_{13} + \phi - \Delta k_3z) \\ & - g'\sqrt{I_1I_4}[\cos(\phi_{12} + \phi_{42} + \Delta k_3z + 3\phi) + \cos(\phi_{12} + \phi_{42} + \Delta k_3z - \phi)] \\ & - g'\frac{\sqrt{I_2I_3I_4}}{I_1}[\cos(\phi_{31} + \phi_{42} - 2\phi + 2\Delta k_3z) + \cos(\phi_{31} + \phi_{42} + \phi + 2\Delta k_3z)], \end{aligned} \quad (19)$$

$$\begin{aligned} \frac{d\phi_3}{dz} = & -g'(I_3 + 2I_1 \cos\phi + 2I_2 \cos\phi + 2I_4 \cos 3\phi) - gI_1\frac{\sqrt{I_2}}{I_3} \cos(\phi_{13} + \phi_{12} - \phi - \Delta k_3z) \\ & - g'\frac{\sqrt{I_1I_2I_4}}{I_3}[\cos(\phi_{13} + \phi_{24} - \phi - 2\Delta k_3z) + \cos(\phi_{13} + \phi_{24} - 2\phi - 2\Delta k_3z)], \end{aligned} \quad (20)$$

$$\begin{aligned} \frac{d\phi_4}{dz} = & -g'(I_4 + 2I_1 \cos 2\phi + 2I_2 \cos\phi + 2I_3 \cos 3\phi) - gI_2\frac{\sqrt{I_1}}{I_4} \cos(\phi_{21} + \phi_{24} + \phi - \Delta k_3z) \\ & - g'\frac{\sqrt{I_1I_2I_3}}{I_4}[\cos(\phi_{13} + \phi_{24} + \phi - 2\Delta k_3z) + \sin(\phi_{13} + \phi_{24} + 2\phi - 2\Delta k_3z)]. \end{aligned} \quad (21)$$

where $g' = (g/2)\sqrt{\epsilon/\mu}$.

It is obvious that the preceding theory can be generalized to include higher-order diffractions, e.g., as done in Ref. 14 using the complex field amplitude approach. However, the preceding four-wave interaction model is sufficient to describe practically all the basic physics.

THEORETICAL DISCUSSIONS AND NEW NUMERICAL RESULTS

In the form of the coupled real amplitude-and-phase equations (8)–(15), the evolution of, and energy ex-

changes among the pump, the probe, and the diffracted beam as a function of the interaction length, the intensity, and the various phase factors (phase shifts, phase mismatches), etc. can be clearly tracked. As previously noted, the terms on the right-hand side (r.h.s.) of Eqs. (8)–(15) consist basically of two types of terms. Terms of the so-called two-wave-mixing type are grouped into the first line on the r.h.s. These terms depend neither on the phase shifts among the beams (ϕ_{21}, ϕ_{31} , etc.), nor on the phase mismatch. However, they are critically dependent on the phase shift ϕ (between the intensity and the index gratings). Such phase shifts can occur naturally in photorefractive materials, or in Kerr media subject to moving intensity grating.¹⁵ If the phase mismatch (arising from the integrated response of the terms containing $\Delta k_3 z$) is large, which happens if the interaction length is long or the pump-probe crossing angle is large, then I_3 and I_4 will be of diminishing amplitude, and we will recover the usual equations describing two wave mixings

$$\frac{dI_1}{dz} = -4g \sin\phi I_1 I_2 - \alpha I_1, \quad (22)$$

$$\frac{dI_2}{dz} = 4g \sin\phi I_1 I_2 - \alpha I_2, \quad (23)$$

$$\frac{d\phi_1}{dz} = -g(I_1 + 2I_2 \cos\phi), \quad (24)$$

$$\frac{d\phi_2}{dz} = -g(I_2 + 2I_1 \cos\phi). \quad (25)$$

Obviously, if $\phi = 90^\circ$, there is a maximum *unidirectional* flow of energy from beam 1 to beam 2, irrespective of which beam is stronger. This two-wave-mixing process is the basic mechanism for work on phase conjugation, wave mixing, self-pumped oscillations, image amplification, etc. in photorefractive materials.

If the medium is thin, and/or the pump-probe crossing angle is small, such that there is negligible phase mismatch, then all the remaining terms on the r.h.s. of (14)–(21) will contribute, and the interactions among the beams become much more complicated and interesting. Some aspects of this multiwave mixing were discussed in a previous article.¹⁴ In the present formalism, in terms of phase and amplitude, further interesting insights into this seemingly untractable coupling among the beams can be obtained. The situation becomes particularly clear if we deal with a Kerr-like medium ($\phi = 0$) with the following redefinitions:

$$\begin{aligned} \Phi_1(x) &= \phi_{12}(z) + \phi_{13}(z) - \Delta k_3 z, \\ \Phi_2(z) &= \phi_{12}(z) + \phi_{42}(z) + \Delta k_3 z, \\ \Phi_3(z) &= \phi_{31}(z) + \phi_{42}(z) + 2\Delta k_3 z. \end{aligned} \quad (26)$$

Note that $\Phi_3 = \Phi_2 - \Phi_1$.

Equations (14)–(17) for the intensity become

$$\begin{aligned} \frac{dI_1}{dz} &= -\alpha I_1 - 4g I_1 \sqrt{I_2 I_3} \sin\Phi_1 - 2g I_2 \sqrt{I_1 I_4} \sin\Phi_2 \\ &\quad + 4g \sqrt{I_1 I_2 I_3 I_4} \sin\Phi_3, \end{aligned} \quad (27)$$

$$\begin{aligned} \frac{dI_2}{dz} &= -\alpha I_2 + 2g I_1 \sqrt{I_2 I_3} \sin\Phi_1 + 4g I_2 \sqrt{I_1 I_4} \sin\Phi_2 \\ &\quad + 4g \sqrt{I_1 I_2 I_3 I_4} \sin\Phi_3, \end{aligned} \quad (28)$$

$$\frac{dI_3}{dz} = -\alpha I_3 + 2g I_1 \sqrt{I_2 I_3} \sin\Phi_1 - 4g \sqrt{I_1 I_2 I_3 I_4} \sin\Phi_3, \quad (29)$$

$$\frac{dI_4}{dz} = -\alpha I_4 - 2g I_2 \sqrt{I_1 I_4} \sin\Phi_2 - 4g \sqrt{I_1 I_2 I_3 I_4} \sin\Phi_3, \quad (30)$$

and the equations for the phases (18)–(21) become

$$\begin{aligned} \frac{d\Phi_1}{dz} &= -g(I_1 + 2I_2 + 2I_3 + 2I_4) - g I_2 \sqrt{I_4/I_1} \cos\Phi_2 \\ &\quad - 2g \sqrt{I_2 I_3} \cos\Phi_1 - 2g \sqrt{I_2 I_3 I_4/I_1} \cos\Phi_3, \end{aligned} \quad (31)$$

$$\begin{aligned} \frac{d\Phi_2}{dz} &= -g(I_2 + 2I_1 + 2I_3 + 2I_4) - g I_1 \sqrt{I_3/I_2} \cos\Phi_1 \\ &\quad - 2g \sqrt{I_1 I_4} \cos\Phi_2 - 2g \sqrt{I_1 I_3 I_4/I_2} \cos\Phi_3, \end{aligned} \quad (32)$$

$$\begin{aligned} \frac{d\Phi_3}{dz} &= -g(I_3 + 2I_1 + 2I_2 + 2I_4) - g I_2 \frac{\sqrt{I_2}}{I_3} \cos\Phi_1 \\ &\quad - 2g \frac{\sqrt{I_1 I_2 I_4}}{I_3} \cos\Phi_3, \end{aligned} \quad (33)$$

$$\begin{aligned} \frac{d\Phi_4}{dz} &= -g(I_4 + 2I_1 + 2I_2 + 2I_3) - g I_2 \frac{\sqrt{I_1}}{I_4} \cos\Phi_2 \\ &\quad - 2g \frac{\sqrt{I_1 I_2 I_3}}{I_4} \cos\Phi_3. \end{aligned} \quad (34)$$

The generation of the diffracted beams 3 and 4, the amplification (or deamplification) of beam 2, and the evolution of the phases, phase shifts, and intensity-dependent phase shifts are shown to be described simply by the two inputs $I_1(0)$ and $I_2(0)$, and the phase shift combinations Φ_1 , Φ_2 , and Φ_3 . The initial values for $I_1(0)$ and $I_2(0)$ are the input pump and probe beam intensities to be chosen in the experiment. The initial values for Φ_1 , Φ_2 , and Φ_3 are $\Phi_1(0) = \pi/2$, $\Phi_2(0) = -\pi/2$, and $\Phi_3(0) = \pi$ rad, respectively. The setting of these phases is governed by physical conditions at the $Z = 0$ plane. Consider, for example, Eq. (33) for Φ_3 . Multiplying both the r.h.s. and the l.h.s. by I_3 and noting that at $Z = 0$, $I_3 = I_4 = 0$, we get

$$\cos\phi_1(0) = 0.$$

This means that $\Phi_1(0) = \pm\pi/2$. Similarly, multiplying both the l.h.s. and r.h.s. of Eq. (28) Φ_4 and noting that $I_4 = 0$ and $I_3 = 0$ at $Z = 0$, we get

$$\cos\Phi_2(0) = 0,$$

i.e.,

$$\Phi_2(0) = \pm\pi/2.$$

If we further note that the wave-mixing contribution to

I_3 and I_4 gives rise to positive dI_3/dz and dI_4/dz , then $\Phi_1(0)$ must be chosen to be $\pi/2$ and $\Phi_2(0) = -\pi/2$, unambiguously.

Once these initial values for the Φ 's and I 's are known, the subsequent growth and energy interchanges among the beam can be seen by calculating the z dependence of the Φ and I from Eqs. (27)–(34) above. Consider Figs. 2, 3, and 4, which are respective plots of Φ_1 , Φ_2 , and Φ_3 as a function of the distance z into the nonlinear medium. For this calculation we have used parameters close to what may be realized in actual experiments. [The crossing angle θ between beam 1 and 2 is set at 0.001 rad, $\lambda = 0.5145 \mu\text{m}$, $I_1(0) = 20 \text{ W/cm}^2$; $I_1(0)/I_2(0)$, the beam ratio, is 100; the linear loss α is 20 cm^{-1} and the nonlinear coefficient $n_{21} = 2.26 \times 10^{-4} \text{ cm}^2/\text{W}$.]

For small θ , the phase mismatch $\Delta k \cong k\theta^2/2$, which, though small, does contribute to a few degrees in phase shift for film thickness exceeding $100 \mu\text{m}$.

Figure 2 shows that for $d = 0$ – $500 \mu\text{m}$, Φ_1 starts from 90° and increases to 160° quite rapidly, then begins to “saturate” for $d \gtrsim 200 \mu\text{m}$. Since $\sin \Phi_1$ for this range of Φ_1 is positive, the term in Eq. (28) $2gI_1\sqrt{I_2I_3}\sin\Phi_1$ will be positive throughout, and contribute positively as a gain channel for the probe (I_2) gain.

On the other hand, Fig. 3 shows how Φ_2 , which is initially -90° , increases very rapidly to about 0 and begins to saturate at this value for $d \gtrsim 200 \mu\text{m}$. From $d = 0$ – $500 \mu\text{m}$, Φ_2 therefore remains negative, and therefore the term $4gI_2\sqrt{I_1I_4}\sin\Phi_2$ in Eq. (28) for the probe beam will be negative, contributing therefore a *loss channel* for the probe beam.

Since $\Phi_3 = \Phi_2 - \Phi_1$, from the results of Figs. 2 and 3, Φ_3 is not expected to change much. Figure 4 is a plot of $\Phi_3(z)$ with the vertical scale highly expands. It shows that $\Phi_3(0)$ rises from -180° to -160° very rapidly between $d = 0$ and $d = 60 \mu\text{m}$. It then drops to about 167° (at $d = 300 \mu\text{m}$) gradually and stays around there. Therefore, $\sin\Phi_3$ practically stays small and negative.

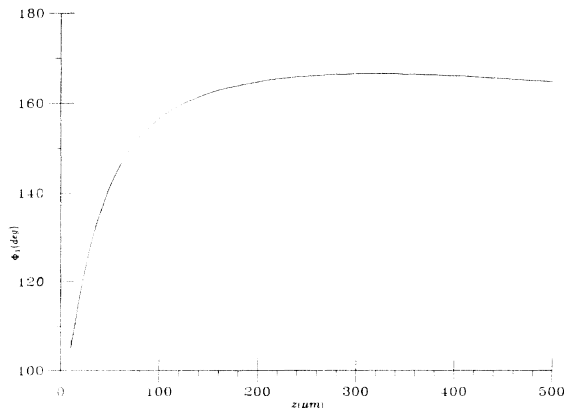


FIG. 2. Plot of the phase Φ_1 (vertical axis in degrees), as a function of the distance z (in micrometers) into the nonlinear medium.

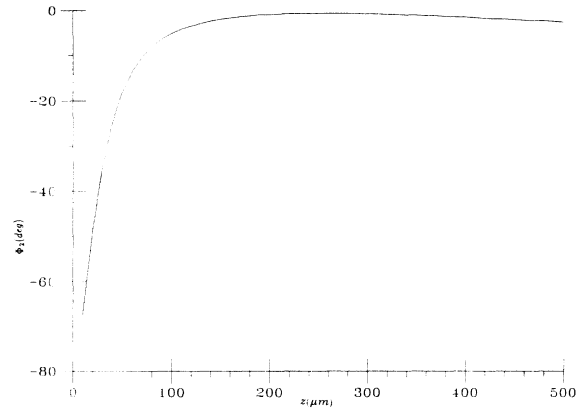


FIG. 3. Plot of the phase Φ_2 (vertical axis in degrees) as a function of the distance z (in micrometers) into the nonlinear medium.

From these results, and from Eqs. (27)–(30), we would expect that most of the “growth” of I_3 and gain of I_2 will take place in the first $200 \mu\text{m}$ or so before losses (from α) and these phase shifts begin to “stunt” the growth. Figure 5 shows the *gain of the probe beam* $I_2(d)/I_2(0)$ and clearly illustrates this point. The drop in the probe gain for $d > 300 \mu\text{m}$ is due to the medium loss, which may be more clearly seen in Fig. 6, which plots out beam-1–beam-4 intensities as functions of the medium thickness. For $d \gtrsim 200 \mu\text{m}$ the pump beam intensity has dropped to $\approx 25\%$ of input value. As a matter of fact, for $d > 380 \mu\text{m}$, I_1 is much less than I_3 or I_2 [due to a combination of linear losses (α) and a diffraction (wave mixing) loss to I_2 and I_3].

For the particular set of values used in getting these plots, one may conclude, therefore, that $300 \mu\text{m}$ is the optimal thickness, and the maximal probe beam

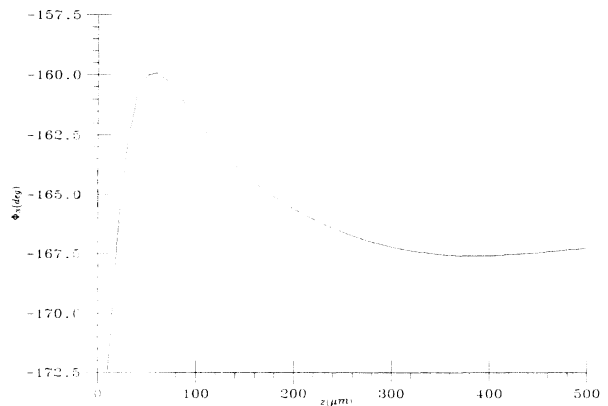


FIG. 4. Plot of the phase Φ_3 (vertical axis in degrees) as a function of the distance z (in micrometers) into the nonlinear medium.

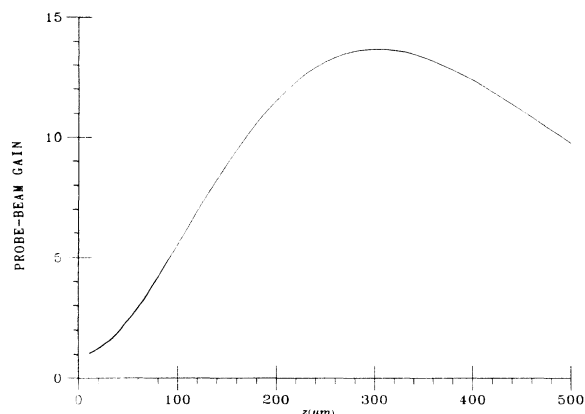


FIG. 5. Plot of the probe beam gain $I_2(z)/I_2(0)$ as a function of the distance z (in micrometers) into the nonlinear medium.

amplification is about 13. Obviously, if α , n_2 , and/or $I_1(0)$ and the ratio $I_1(0)/I_2(0)$ are changed, the results are different. For the same α and n_2 , it is possible to get a probe gain as high as 100 at a pump-probe ratio of 1000.

EFFECT OF NONLOCAL RESPONSE ($\phi \neq 0$)

The preceding discussions on the effect of the laser phase apply to the so-called local nonlinear response case (i.e., the phase shift ϕ between the intensity grating and the index grating is zero). This is true in a Kerr-like medium if the frequencies of the pump and the probe beam are the same. If there is a detuning between the two beam frequencies, giving rise to a moving intensity grating on the nonlinear medium, the resulting refractive index grating will be relatively phase shifted (i.e., $\phi \neq 0$) with respect to the intensity grating. Alternatively, one

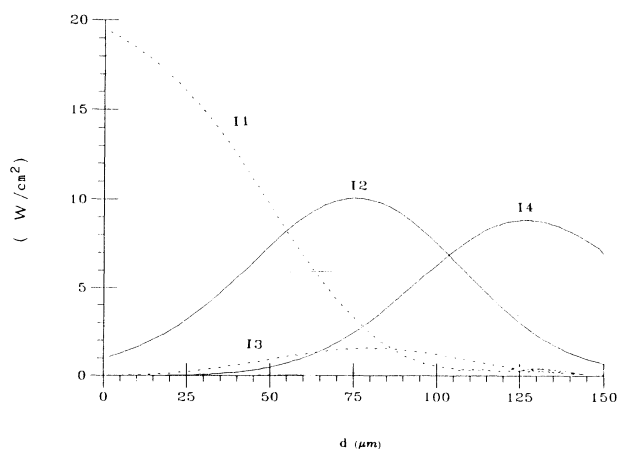


FIG. 6. Plots of all incident and generated beams as a function of the nonlinear-medium thickness (in micrometers).

can translate the nonlinear medium along the $\Delta\mathbf{K}=\mathbf{K}_1-\mathbf{K}_2$ direction to create the same nonlocal response.

If $\phi \neq 0$, then we have to go back to solving the set of equations (14)–(21), rather than the simpler set of equations (27)–(34). Nevertheless, it is possible to get some physical insights by considering and comparing (15) for dI_2/dZ (in the case of $\phi \neq 0$) and Eq. (28) for dI_2/dZ (for $\phi = 0$).

The major contributor of the growth of the probe intensity I_2 (for $\phi = 0$) for Eq. (28) is the term $2gI_1\sqrt{I_2I_3}\sin\phi_1 = T_0$. On the other hand, from Eq. (15), the major contributor is

$$4gI_2I_1\sin\phi + 2gI_1\sqrt{I_2I_3}\sin(\phi_1 + \phi) = T_1.$$

If $\phi \neq 0$, the two-wave-mixing terms $4gI_2I_1\sin\phi$ in T_1 will contribute positively (for $\phi > 0$) or negatively (for $\phi < 0$) to the probe-beam growth. On the other hand, $(\phi_1 + \phi)$ will increase from $\pi/2$ (if $\phi = 0$) or decrease from $\pi/2$ (if $\phi < 0$). The contribution of the four-wave-mixing term $2gI_1\sqrt{I_2I_3}\sin(\phi_1 + \phi)$ in T_1 therefore, is still positive. Consequently, if $\phi > 0$, the probe beam will experience a higher gain than if $\phi = 0$. On the other hand, if $\phi < 0$, the two-wave-mixing term $4gI_2I_1\sin\phi$ will contribute negatively to the probe-beam intensity, although the four-wave-mixing term $2gI_1\sqrt{I_2I_3}\sin(\phi_1 + \phi)$ is still positive. In this case, one would expect a decrease in the overall probe gain.

When higher-order diffracted beams of substantial magnitude are present, the interplay between these phases and phase shifts becomes very complicated. Nevertheless, both the numerical calculations and our experimental results confirm the preceding qualitative observations.⁴

EXPERIMENTS

The theory discussed in the preceding sections applies generally to any nonlinear medium, and thus the choice of performing beam (or image-bearing beam) amplification is dictated by the intended application or fundamental pursuit. In this section we will summarize some of the experimental results obtained using nematic liquid-crystal film as the nonlinear film. Observation of probe-beam gain and comparison with theory that accounts for other relevant physical parameters (e.g., medium's intensity-dependent loss, diffusion, etc.) have also been done in other studies.^{4,14} In this paper we will present hitherto unreported results based on the orientational nonlinearity of liquid crystals.

From previous studies,⁸ it is well known that as a result of laser induced reorientation of the nematic director axis (a birefringent material), there is a large accompanying intensity-dependent refractive index change. For a 100- μm thick sample, with the linearly polarized laser incident at an external angle of 45° to the sample (i.e., at an angle $\theta_i \approx 22^\circ$ between \mathbf{k} and \mathbf{n}), the typical nonlinear coefficient $n_{2I} \approx 2 \times 10^{-4} \text{ cm}^2/\text{W}$ (c.f., Ref. 8). [Actually the nonlinear response of the liquid-crystal reorientation is z dependent, which means the coupling constant g is

also a function of z . This dependence can be easily incorporated in the numerical solution of Eqs. (14)–(21). We found that the solutions using this more detailed dependence of g and an average value of g are not appreciably different.]

The experiments are performed using a linearly polarized argon-ion laser operating at the 5145-Å line. The laser is split into a pump and a probe beam (with the pump-probe beam ratio an adjustable experimental parameter). To investigate thickness dependence, up to nine layers of 100- μm nematic films are stacked together, each film separated from the other by a very thin glass plate.

In all the experimental measurements, the liquid crystal used is (PCB) (K15 from EM Chemicals pentylcyano-biphenyl) at room temperature. Occasionally, we also used E46 (from EM Chemicals) and obtained similar results. As a result of the large nonlinearity in combination with the (Gaussian) beam size (about 1-mm diameter for the probe and 2-mm diameter for the pump), self-modulation and external self-focusing and the resulting increased divergence and rings formation are experienced by all the transmitted beams (mostly due to pump-induced refraction-index change) for pump power $\gtrsim 100$ mW. At the highest power used in these experiments, there are two visible diffractions (beams 3 and 4) if the probe beam is weak (pump-probe ratio > 20). If equal pump and probe beam powers are used, second-order diffracted beams are clearly visible. The increased divergence can exceed the crossing angle θ and the output beams can no longer be individually measured accurately. Quantitative comparison with theory can therefore be made only in the *low-power–low-gain regime*.

Figure 7 shows the experimentally observed probe gain as a function of the pump-probe beam ratio obtained at a pump-beam power of 33 mW. As expected, there is no gain if the pump and the probe beams are of equal intensity. As the pump-probe intensity ratio increases, the probe gain increases, in very good agreement with theory (dashed line). The gain saturates at about 30% above a

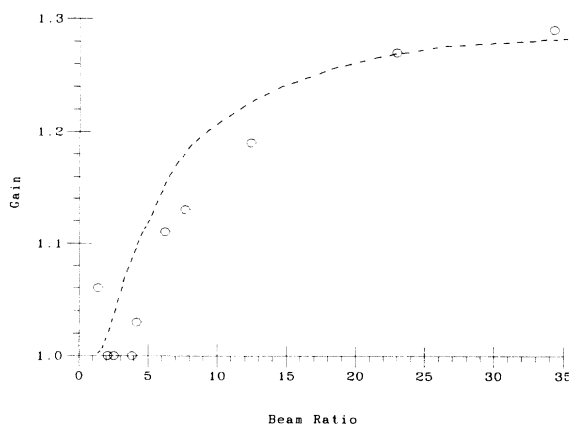


FIG. 7. Experimentally observed probe gain as a function of the pump-probe intensity ratio.

ratio of > 35 . Much higher gain can be obtained by increasing the pump-beam intensity, and/or using a thicker nematic liquid-crystal film as shown in Fig. 8, where a pump-probe beam ratio of 208 is used. Gain as high as 250% can be achieved with a pump intensity on the order of 15 W/cm^2 in a 152- μm -thick nematic liquid-crystal film. At these power levels, the diffracted beams 3 and 4 are clearly visible, but they are quite weak compared to the probe (and of course, to the pump) to cause a decrease in the probe gain. This is shown by the excellent agreement between the theory (solid line) and the experimental results (circle). In the same figure we have also plotted the *effective gain* (in triangles) defined as $[I_2(d)$ with pump] $/[I_2(d)$ without pump], and the corresponding theory. The value of n_{21} that fits these curves is about $5 \times 10^{-5} \text{ cm}^2/\text{W}$, which is expected of a 152- μm -thick nematic liquid-crystal film.

Since the nonlinearity of nematic liquid-crystal film is a function of the film thickness, it is not possible to study the thickness dependence of the probe gain or the diffraction efficiency by using samples of different thickness. Experimentally, we have studied the thickness dependence by using multiple (closely stacked) layered nematic liquid-crystal films; each layer is about 100 μm thick and is separated from one another by a thin ($< 100\text{-}\mu\text{m}$) glass plate. Samples up to nine layered films of good optical quality have been made. By studying probe-beam gain or diffraction efficiency in different layered samples, a good insight into the role of absorption loss may be gained. Figure 9 is the observed probe-beam gain as a function of the number of liquid-crystal layers. The experimental results (circles) show that as the number of layers increase, the probe-beam gain first increases and then drops off rather quickly. The drop in the probe-beam gain is due primarily to the loss (α), which has been measured in a separate experiment to be on the order of 20 cm^{-1} . This is evident if we plot the experimentally observed effective gain as a function of the number N of layers used (Fig. 10). The effective gain (i.e.,

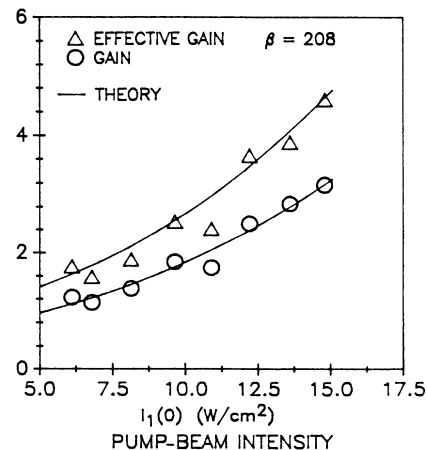


FIG. 8. Experimentally observed probe gain dependence on the pump-beam intensity.

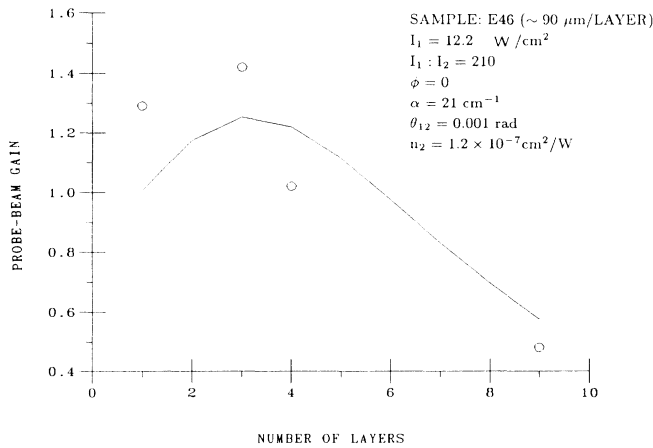


FIG. 9. Experimentally observed probe-beam gain as a function of the number of nonlinear nematic film layers. Each layer is $100 \mu\text{m}$ thick. Solid line is theoretical curve.

with the loss α removed) in general increases as N increases. Both Figs. 9 and 10 can be fitted qualitatively well with our theory using $n_{2I} \approx 1.1 \times 10^{-5} \text{ cm}^2/\text{W}$, and the experimental parameters of $\beta = 208$, $I_1 = 10 \text{ W}/\text{cm}^2$ crossing angle $\theta \approx 0.001 \text{ rad}$, and $\alpha = 20 \text{ cm}^{-1}$.

At a large pump-probe beam ratio β , the diffracted beam I_3 is quite weak. By lowering β to about 5, diffraction (I_3) is easily visible, and can be accurately measured. The results are depicted in Fig. 11, where the diffraction efficiency is plotted as a function of the number of layers. In general, because of the larger signal (compared to the background noise), the data in Fig. 11 shows less "scattering" than those in Fig. 9 and 10. The theoretical curve using parameter quoted above with $I_1/I_2 \approx 5$ fits the data very well. Again, we note that the drop in the diffraction efficiency at higher N values is due to the medium loss. In nematic liquid crystals, these

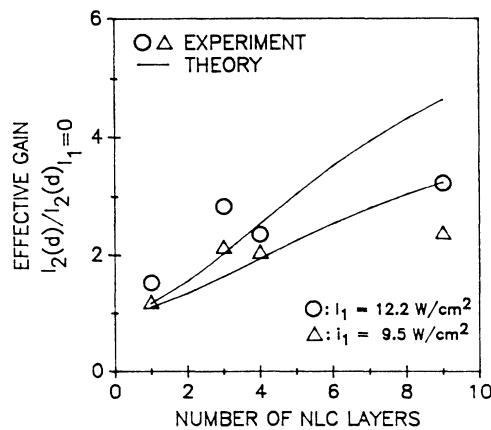


FIG. 10. Experimentally observed effective gain as a function of the number of nonlinear nematic layers. Circle: experiment; solid curve: theory.

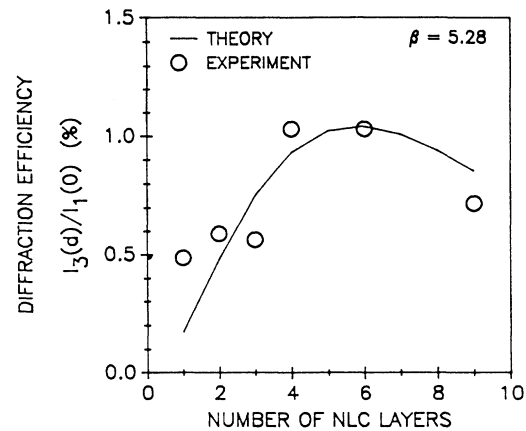


FIG. 11. Observed diffraction (beam 3) efficiency as a function of number of nematic layers.

scattering losses are highly wavelength dependent (drop off faster than λ^{-2}). We therefore expect that these probe amplifications and other wave-mixing processes will be very efficient in the infrared and far-infrared regime. Indeed, using a CO_2 laser and a totally different kind of nonlinearity (diffusive thermal nonlinearity in liquid crystals), we have observed probe gain as large as 20 or more.^{4(b)}

Experimentally, we have also investigated the effect of nonlocal response in the probe amplification using two methods: (i) by imparting a frequency offset between the pump and the probe beams, accomplished by translating one of the mirror directing the probe beam to the sample, and (ii) by translating the sample in the direction of the grating wave vector $\mathbf{k}_1 - \mathbf{k}_2$. Both methods yield the same results. Figure 12 shows the observed probe gains plotted as function of the wave mixings angle (which affect the nonlinearity constant n_{2I}). In general, the gain decreases with increasing value of the mixing angle, in ac-

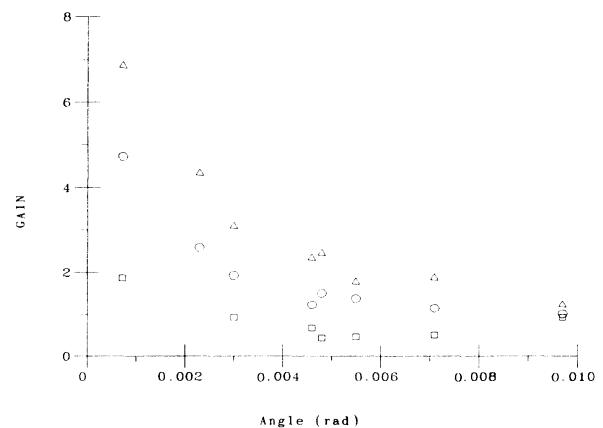


FIG. 12. Plots of the experimentally observed probe-beam gain as a function of the wave-mixing angles for probe beams that are (a) circles: non-shifted; (b) triangles: Stokes-shifted; and (c) squares: anti-Stokes-shifted.

cordance with previously studied dependence of the re-orientational nonlinearity on the wave-mixing angle.⁹ The triangles are obtained for a probe beam that is Stokes shifted (i.e., lower frequency compared to the pump); equivalently, the sample is translated in the $\mathbf{k}_1 - \mathbf{k}_2$ direction. In general, there is an increased probe gain compared to the nonshifted case (data in circles) in agreement with the theoretical expectation discussed earlier. On the other hand, squares are data for the case of an anti-Stokes-shifted probe beam, and generally the probe-beam gain is diminished. The absolute values of the relative increase or decrease in the probe-beam gain depend on the magnitude of the frequency shift (which depends on the velocity of the mirror directing the probe beam to the sample), or the velocity of translation of the sample. Due to the limitation in our instrumentation, the absolute value of these speeds cannot be accurately measured. The results obtained in Fig. 12 (for the Stokes- and anti-Stokes-shifted probe beam) correspond to the *maximal* observed increases or decreases in the nonshifted probe-beam gain as these speeds are varied. In our numerical computations, the value for ϕ is varied from 0 to $\pm\pi/2$, and we have found that the *maximal* changes in the probe gain (for $\phi > 0$ and $\phi < 0$ corresponding to Stokes and anti-Stokes shiftings, respectively) are in good agreement with these experimentally observed values.

CONCLUSION

A theory of multiwave mixing is developed to describe some newly observed probe-beam amplification in a Kerr-like medium. The coupled amplitude and phase equations account for all relevant parameters such as intensities, intensity-dependent phase shifts, phase mismatches, and beam intensity ratios. They can also be generalized to describe non-Kerr-like media where a finite phase shift exists between the intensity and the induced refractive index gratings. By further including the intensity-dependent medium loss, the theory can also be applied to processes where the laser-induced nonlinear mechanism introduces new losses experienced by the beam, as in the case of laser-induced electron-hole plasma in semiconductors.^{5(b)} Experiments have been performed in nematic liquid-crystal films which possess large orientational nonlinearity, and the observed probe-beam gain dependence on the pump-probe ratio, on film thickness, on the pump intensity, and nonlocal phase shift, etc. are in good agreement with the theory.

ACKNOWLEDGMENTS

This research is supported by National Science Foundation Grant No. ECS 8712078.

*Present address: Jet Propulsion Laboratory, California Institute of Technology, Pasadena, CA 91125.

¹See, for example, *Optical Bistability III*, edited by H. M. Gibbs, P. Mandel, N. Peyghambarian, and S. D. Smith (Springer-Verlag, Berlin, 1986).

²See, for example, all the articles on the special issue *Opt. Eng.* **24**, (1985).

³G. Pauliat, J. P. Huignard, A. Delboulbe, G. Rossen, and J. P. Huignard, *J. Opt. Soc. Am. B* **3**, 307 (1986), and references therein.

⁴(a) I. C. Khoo and T. H. Liu, *IEEE J. Quant. Electron.* **QE-23**, 171 (1987); (b) I. C. Khoo, P. Y. Yan, G. M. Finn, T. H. Liu, and R. R. Michael, *J. Opt. Soc. Am. B* **5**, 202 (1988).

⁵(a) H. J. Eichler, M. Glotz, A. Kummrow, K. Richter, and X. Yang, *Phys. Rev. A* **35**, 4673 (1987); (b) I. C. Khoo and R. Normandin, *Appl. Phys. Lett.* **52**, 525 (1988).

⁶See, for example, J. F. Reintjes, *Nonlinear Optical Parametric Processes in Liquid and Gases* (Academic, New York, 1984),

and references therein on degenerate wave mixings.

⁷M. B. Klein, *Opt. Lett.* **9**, 350 (1984).

⁸B. Fischer, J. O. White, M. Cronin-Golomb, and A. Yariv, *Opt. Lett.* **11**, 239 (1986).

⁹G. C. Valley, *J. Opt. Soc. Am. B* **1**, 868 (1984).

¹⁰V. L. Vinetskii, N. V. Kukhtarev, S. G. Odulov, and M. S. Soskin, *Usp. Fiz. Nauk.* **129**, 113 (1979) [*Sov. Phys.-Usp.* **22**, 742 (1979)], and references therein.

¹¹V. L. Vinetskii, N. V. Kikhtarev, and M. S. Soskin, *Kvant Electron. (Moscow)* **4**, 420 (1977) [*Sov. J. Quant. Electron.* **7**, 230 (1971)].

¹²L. Richard, J. Maurin and J. P. Huignard, *Opt. Commun.* **57**, 365 (1986).

¹³Pochi Yeh, *J. Opt. Soc. Am. B* **3**, 747 (1986).

¹⁴See, for example, I. C. Khoo, *Nonlinear Optics of Liquid Crystals*, Vol. XXVI of *Progress in Optics*, edited by E. Wolf (North-Holland, Amsterdam, 1988).

¹⁵I. C. Khoo, *Phys. Rev. A* **27**, 2747 (1983).